

Stability of metal-rich massive stars

Christopher J. White^{1*} and J. Goodman¹

¹*Princeton University Observatory, 4 Ivy Lane, Princeton, NJ, 08544, U.S.A.*

Submitted 2014 March

ABSTRACT

We revisit the stability of very massive main-sequence stars at solar metallicity, with the goal of understanding whether pulsations set a physical upper limit to stellar mass. Models of up to 938 solar masses are constructed with the MESA code, and their radial linear stability analysed with a nonadiabatic method following that of Castor. Despite uncertainty about the effects of convection on the linear growth rate, we conclude that even if the fundamental radial mode is unstable, the growth rate will be small. Consequently the amplitude at nonlinear saturation will also be small and not dangerous to the star. We demonstrate this for our most massive model by estimating the nonlinear parametric coupling to short-wavelength g modes. Although our stellar models are hydrostatic, the structure of their outer parts suggests that optically thick, radiatively driven winds are more likely to limit the main-sequence lifetime.

Key words: stars: massive – asteroseismology – instabilities

1 INTRODUCTION

The threshold of hydrogen burning ($\approx 0.08 M_{\odot}$) is generally accepted as a physical lower limit to the masses of stars, one that is independent of the environment in which stars form. Whether there is a definite upper limit to stellar masses, and to what extent the limit may depend on nature (stellar physics) or nurture (star-forming environment), are open questions. The highest well-measured dynamical masses are $\sim 80 M_{\odot}$ (Schnurr 2012), most notably the double-lined eclipsing binary WR 20a (Rauw et al. 2004; Bonanos et al. 2004). Statistics of stars in galactic open clusters have been interpreted as evidence for an upper limit $\sim 150 M_{\odot}$ (Weidner & Kroupa 2004; Oey & Clarke 2005; Figer 2005; Koen 2006), while Crowther et al. (2010) present spectroscopic arguments for larger masses among the stars in the cluster R136 of the Large Magellanic Cloud. An empirical mass limit, if such exists, may reflect the environment in which most stars are observed to form – that is to say, molecular clouds – where the density of hydrogen nuclei is typically $n \lesssim 10^3 \text{ cm}^{-3}$, the temperature $\lesssim 100 \text{ K}$, and dust is abundant – rather than physics intrinsic to the star once formed.

One of us has previously argued that the broad-line regions of bright QSO accretion disks are likely selfgravitating and prone to form very massive stars – at least several hundred solar masses at the onset of gravitational instability, and perhaps $\gtrsim 10^5 M_{\odot}$ after accretion up to the isolation mass (Goodman & Tan 2004; Jiang & Goodman 2011).

Whatever one makes of the dynamical arguments, it is clear that a QSO disk at $\sim 10^3$ gravitational radii from the black hole is a very different environment from a molecular cloud: the ambient density is orders of magnitude higher and the dynamical timescale correspondingly shorter, the temperature is above the sublimation point for dust, rotation and shear are strong, turbulence is probably subsonic, and radiation pressure may exceed gas pressure. Hence if stellar masses are sensitive to their natal environment, a different maximum stellar mass might result in such disks than in giant molecular clouds. On the other hand, it is well known that very massive stars are fragile due to the predominance of radiation over gas pressure ($P_{\text{rad}}/P_{\text{gas}} \propto M^{1/2}$ at $M \gtrsim 100 M_{\odot}$), radiatively driven winds, and pulsational instabilities. Thus it is possible that internal physics establishes an upper limit $\lesssim 10^2\text{--}10^3 M_{\odot}$. A presumably fatal relativistic instability sets in above $10^5\text{--}10^6 M_{\odot}$, depending upon internal rotation (Chandrasekhar 1964; Baumgarte & Shapiro 1999; Montero et al. 2012, and references therein). This leaves a gap of several orders of magnitude above the largest observed masses, however.

In the present paper, we return to the question of pulsational instabilities driven by the κ - and ϵ -mechanisms, which are sensitive to composition via opacities and to nuclear reaction rates. This is a problem that has been considered by many authors since the original work by Schwarzschild & Härm (1959), and one might have thought it a closed subject. However, the understanding of the input physics, notably the opacities, has evolved while the effects of convection on the linear growth rates remain uncertain,

* E-mail: cjwhite@princeton.edu (CJW)

as do the mechanisms responsible for nonlinear saturation of the pulsations if they grow at all.

Recently, Shiode et al. (2012, hereafter SQA) have revisited the ϵ -mechanism. Applying a quasi-adiabatic analysis to equilibrium models constructed with the MESA code (Paxton et al. 2011, 2013), they concluded that the instability is suppressed by the effective viscosity due to turbulent convection, at least for stars of masses $\lesssim 1000 M_\odot$. However, they did not consider any models above $100 M_\odot$ with solar or higher metallicity. Since QSO disks appear to be metal rich, with metallicities perhaps up to ten times solar (Hamann & Ferland 1999; Dietrich et al. 2003; Matsuoka et al. 2011; Dhanda Batra & Baldwin 2014), one motivation for the present work was to repeat SQA's analysis at higher metallicities *and* masses $> 10^2 M_\odot$. We also wanted to perform a fully non-adiabatic rather than quasi-adiabatic analysis. This is arguably less important for the ϵ -mechanism because it is driven deep within the star where the thermal time is very long. However, SQA also found evidence for instabilities driven by opacity variations in the envelope which they did not fully explore, perhaps because they had less confidence in the quasi-adiabatic approximation for those modes. Also, at least with modern opacities, the envelopes of high-mass stellar models at solar metallicity differ strikingly from those of corresponding Population III models, and this has interesting consequences for the mode structures.

Linear stability analysis is only a first step toward answering the question posed above. If instabilities are found, one must consider how they may saturate in order to decide whether they are likely to shorten the main-sequence lifetime. Early attempts to address the saturation of instabilities driven by the ϵ -mechanism gave conflicting results (Appenzeller 1970; Papaloizou 1973b), but little work has been done along these lines in recent decades. We will argue that even if the uncertain damping effects of convection are neglected, the linear growth rates are so small compared to the real part of the pulsation frequency that the pulsations will saturate by one or another weakly nonlinear mechanism at small amplitudes that do not threaten the survival of these stars, at least not before they have lived out most of the nominal minimum main-sequence lifetime ($\sim 3 \times 10^6$ yr). Instead, looking at the structure of the metal-rich hydrostatic models, as well as a substantial body of work in recent years on Wolf-Rayet and O-star winds, we now believe that radiatively driven mass loss is more likely than pulsational instabilities to limit the lifetimes of the most massive, metal-rich stars. We hope to explore the scaling of the mass-loss timescale (i.e., $|M/\dot{M}|$) with stellar mass in a future paper. Here we merely indicate some of the structural and energetic considerations involved.

The outline of this paper is as follows. Section 2 describes the equilibrium models constructed with MESA. Section 3 discusses our methods for the linear stability analysis, which generally follow the nonadiabatic radial pulsation code of Castor (1971) but with modifications to the outer boundary condition to accommodate high radiation pressure. Results for the modes are given in §4, and a summary of our conclusions and a discussion of future steps follows in §5.

2 METHOD

2.1 Equilibrium Models and Initial Estimates

Like SQA, we generated ZAMS stellar models using the stellar evolution code MESA. Here we highlight the configuration settings used when they deviate from the defaults.

The initial mass is specified, with the initial helium and metal abundances set to $Y = 0.25$ and $Z = 0.02$. The simulation is begun in the pre-main sequence phase, where heat is supplied by gravitational collapse. The atmosphere is modelled as a ‘simple photosphere.’ Convective mixing is implemented following Henyey et al. (1965) in regions determined to be convectively unstable by the Ledoux criterion.

The star is evolved until it is determined to lie on the main sequence, which we here define to be a long-term state in which the total luminosity matches power generated by hydrogen fusion. It should be noted that while MESA has an internal check for when this condition is met, we sometimes run the simulation for more timesteps, especially in the cases of stars above about $100 M_\odot$. This is because the collapsing cloud of material may undergo a small ‘bounce’ in which its gravitational contraction is momentarily halted before resuming.

Once the star has reached its ZAMS phase, the model is saved and the data is analysed with the ADIPLS package (Christensen-Dalsgaard 2008), which computes adiabatic pulsational modes given one-dimensional stellar models. While this package is bundled with MESA and can be integrated into the evolution itself, we run it separately, treating the MESA output as an equilibrium model.

The output from ADIPLS is a set of eigenfrequencies and corresponding mode shapes in the form of radial displacements from equilibrium. We use these outputs in our own routine, which finds mode frequencies and shapes without the adiabatic assumption. We turn to this method now.

2.2 Nonadiabatic Analysis

For the purposes of analysing the pulsational modes in a nonadiabatic framework, we begin with the method outlined in Castor (1971), adding our own extensions where necessary. The star is divided into a set of N concentric mass shells. Modifying the notation used in that paper, the four equations of stellar structure can be written

$$\frac{d^2 r_i}{dt^2} = -\frac{GM_i}{r_i^2} - 4\pi r_i^2 \frac{P_{i+1/2} - P_{i-1/2}}{(M_{i+1} - M_{i-1})/2}, \quad (1)$$

$$T_{i+1/2} \frac{dS_{i+1/2}}{dt} = \frac{L_i - L_{i+1}}{M_{i+1} - M_i} + (\epsilon_{\text{nuc}})_{i+1/2}, \quad (2)$$

$$\frac{1}{\rho_{i+1/2}} = \left(\frac{4\pi}{3} \right) \frac{r_{i+1}^3 - r_i^3}{M_{i+1} - M_i}, \quad (3)$$

$$L_i = \frac{(4\sigma/3)(4\pi r_i^2)^2 (T_{i-1/2}^4 - T_{i+1/2}^4)}{[\kappa_{i+1/2}(M_{i+1} - M_i) + \kappa_{i-1/2}(M_i - M_{i-1})]/2} + (L_{\text{conv}})_i. \quad (4)$$

Here integer subscripts denote quantities evaluated at the interfaces between cells, running from 0 (the central point of the star) out to N (the outer boundary), while half-integer subscripts denote cell-averaged quantities, which can be considered defined at exactly halfway through the mass of the cell. This is a distinction made by Castor and remains con-

ductive to analysing MESA output, as MESA defines intrinsic properties within cells and extrinsic properties at the outer boundaries of cells.

We proceed to take the first-order Lagrangian variations of these equations in radius r , entropy per unit mass S , temperature T , density ρ , pressure P , luminosity L , nuclear energy generation rate per unit volume ε_{nuc} , and opacity κ . Note that M_i , the mass interior to interface i , is constant in the Lagrangian picture. Perturbations to the convective luminosity are neglected, although SQA's quasi-adiabatic recipe for turbulent convective damping is applied in some cases (§4). Time derivatives in the linearized equations are replaced by multiplication by $-\mathrm{i}\omega$, the eigenfrequency ω being complex in general.

The system of equations is closed by choosing four boundary conditions. Following Castor, the inner interface is assumed to be stationary with constant luminosity:

$$\delta r_0 = \delta L_0 = 0. \quad (5)$$

The outer heat equation requires a more general analysis than is given by Castor, as the equations in that work only hold under the assumption that radiation pressure is negligible compared to gas pressure at the outer boundary. This condition clearly does not hold for massive stars. We therefore turn to the equation for radiation pressure in the Eddington approximation,

$$P_{\text{rad}} = \frac{F}{c} \left(\tau + \frac{2}{3} \right), \quad (6)$$

where F is the radiative flux and τ is the optical depth at the location being considered. In terms of more familiar variables, we have

$$P_{\text{rad}} = \frac{L}{4\pi r^2 c} \left(\frac{\kappa \Delta m}{4\pi r^2} + \frac{2}{3} \right), \quad (7)$$

where Δm is the mass exterior to the point being considered. Taking the variation of this equation leads to the result

$$\frac{\delta P_{\text{rad}}}{P_{\text{rad}}} = \frac{\delta L}{L} - 4 \left(\frac{\tau + 1/3}{\tau + 2/3} \right) \frac{\delta r}{r} + \left(\frac{\tau}{\tau + 2/3} \right) \frac{\delta \kappa}{\kappa}. \quad (8)$$

We replace L_{rad} with L here because in practice the model extends far enough into the tenuous atmosphere as to make the contribution of L_{conv} negligible.

When implementing this boundary condition, care should be exercised regarding where the perturbed quantities are evaluated. P_{rad} and κ are naturally defined in the middle of the outermost shell. L and r should be the mass-averaged values of the outermost and penultimate interfaces in the model.

The outer momentum equation is closed as follows. The total pressure at a point near the surface, under a mass Δm and at a radius r , can be written (if the pressure scale height H_P obeys $H_P \ll r$)

$$P = \frac{\Delta m}{4\pi} \left(\frac{\ddot{r}}{r^2} + \frac{GM}{r^4} \right) + \frac{L}{6\pi c r^2}. \quad (9)$$

Subtracting (6) from (9) yields

$$P_{\text{gas}} = \frac{\Delta m}{4\pi} \left(\frac{\ddot{r}}{r^2} + \frac{GM}{r^4} - \frac{\kappa L}{4\pi r^4 c} \right). \quad (10)$$

Perturbing this yields

$$\frac{\delta P_{\text{gas}}}{P_{\text{gas}}} = -\frac{\delta r}{r} \left(4 + \frac{\omega^2 r^3}{\beta GM} \right) - \frac{1-\beta}{\beta} \left(\frac{\delta L}{L} + \frac{\delta \kappa}{\kappa} \right), \quad (11)$$

where β is defined in terms of the Eddington luminosity $L_{\text{Edd}} = 4\pi GMc/\kappa$ by $L = (1-\beta)L_{\text{Edd}}$. One can then express $\delta P_{\text{gas}}/P_{\text{gas}}$ and $\delta L/L$ in terms of the position and entropy variations δr and δS , as for example is done in equations (10) and (11) in Castor (1971). Similarly, the $\delta \kappa/\kappa$ term can be re-expressed using the MESA-supplied values of $(\partial \log \kappa / \partial \log T)|_{\rho}$, $(\partial \log \kappa / \partial \log \rho)|_T$, and other thermodynamic quantities.

Given a stellar model and a (possibly complex) frequency ω , the method outlined above allows us to construct a band-diagonal matrix A_0 such that

$$A_0 \begin{pmatrix} X_{1/2} \\ X_1 \\ \vdots \\ X_{N-1/2} \\ X_N \end{pmatrix} = \begin{pmatrix} \mathrm{i}\omega X_{1/2} \\ \omega^2 X_1 \\ \vdots \\ \mathrm{i}\omega X_{N-1/2} \\ \omega^2 X_N \end{pmatrix}, \quad (12)$$

where

$$X_i = \sqrt{\frac{M_{i+1} - M_{i-1}}{2}} \delta r_i, \quad (13)$$

$$X_{i+1/2} = T_{i+1/2} \delta S_{i+1/2}. \quad (14)$$

Rather than solve this generalized eigenvalue system outright, we note, as Castor did, that the nonadiabatic terms are small enough to be treated as a perturbation. First we rewrite (12) as per (22, 23) of Castor (1971):

$$(G_1 - \omega^2 I) \vec{x} + G_2 \vec{y} = 0, \quad (15)$$

$$K_1 \vec{x} + (K_2 + \mathrm{i}\omega I) \vec{y} = 0. \quad (16)$$

Here G_1 , G_2 , K_1 , and K_2 are band-diagonal $N \times N$ matrices independent of ω . Assume we have an adiabatic eigenvalue ω_0 together with its eigenfunction \vec{x}_0 , such that

$$G_1 \vec{x}_0 = \omega_0^2 \vec{x}_0. \quad (17)$$

Then to first order (cf. (26) of Castor),

$$\omega = \omega_0 - \frac{1}{2\omega_0} \cdot \frac{\vec{x}_0^T G_2 (K_2 + \mathrm{i}\omega_0 I)^{-1} K_1 \vec{x}_0}{\vec{x}_0^T \vec{x}_0}. \quad (18)$$

This reduces to the quasi-adiabatic approximation only if K_2 is neglected.

3 THE SHELF

When MESA evolves massive stars with nonnegligible metallicity, it generically produces an extended envelope outside the polytropic core of the star, as shown in Figures 1 and 2. This extremely diffuse region, incipient at 46 M_{\odot} and distinctly visible by 100 M_{\odot} , occupies a progressively larger fraction of the star's radius but a negligible fraction ($\sim 10^{-5}$) of its mass. Because of its slowly radially varying temperature and density, we call this region the 'shelf.' The opacity in the shelf rises well above the electron-scattering value. Since hydrostatic equilibrium limits the radiative part of the luminosity to the value that just balances gravity, $L_{\text{rad}} = 4\pi GM_* c / \kappa(\rho, T)$, the balance is carried by inefficient and near-sonic convection.

A similar shelf has been observed in models of helium stars (Gräfener et al. 2012, and references therein). While such a layer may dramatically alter the effective temperature

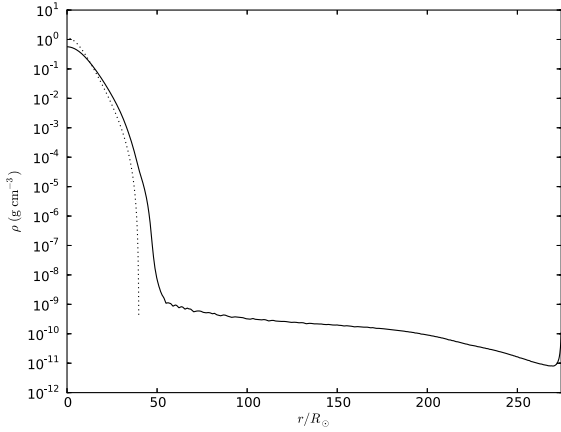


Figure 1. Density in our 938 M_{\odot} model. The dotted line is the density for an $n = 3$ polytrope with radius given by the scaling relation (9) in Goodman & Tan (2004). Note that although considerable in radial extent, the atmospheric shelf has negligible mass compared to the core of the star. This is analogous to Figure 1 in Gräfenner et al. (2012).

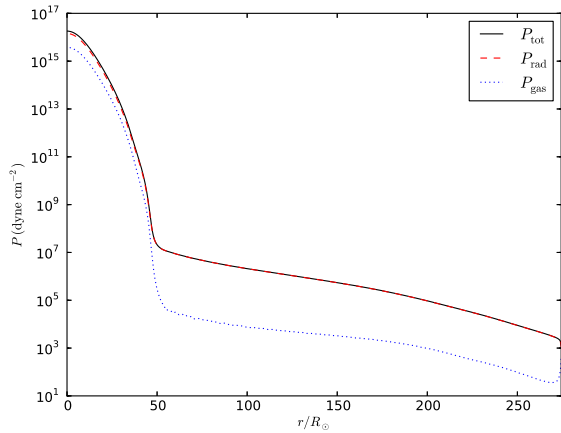


Figure 2. Gas, radiation, and total pressure in our 938 M_{\odot} model. The structure is the same as that shown in Figure 2 in Gräfenner et al. (2012).

and spectrum of the star, we have neglected it in our nonadiabatic pulsational analysis. This is reasonable because its mass is too small to have any considerable impact on the fundamental mode of the core. In fact, it seems likely that the shelf would be replaced by a radiatively driven wind if the constraint of hydrostatic equilibrium was relaxed. This is suggested by the fact that the Bernoulli ‘constant’

$$B = u + \frac{1}{2}v^2 + \frac{P}{\rho} - \frac{GM_r}{r}, \quad (19)$$

becomes positive in the lower part of the shelf, though it changes sign once more in the outer convective regions (Figure 3). Here u is the internal energy per unit mass, and v is the *mean* radial velocity, which of course vanishes in these hydrostatic models. The kinetic energy of the convection would further increase B .

In fact, we were unable to obtain numerical convergence

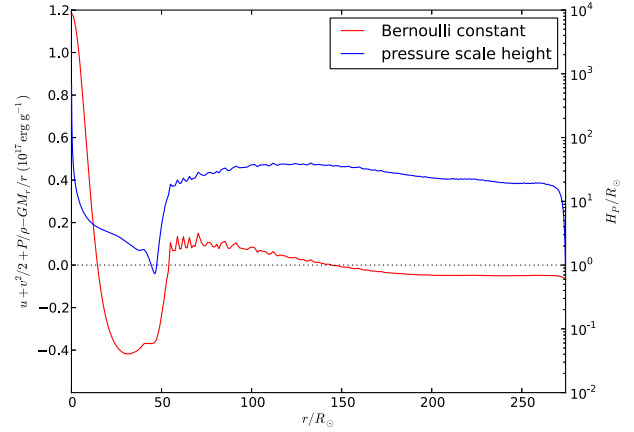


Figure 3. The Bernoulli constant and pressure scale height as a function of radius in our 938 M_{\odot} model. The transition from the core to the extended shelf around 50 solar radii is marked by a sign change in the former and a local minimum in the latter.

for the nonadiabatic modes when the entire shelf was included. The matrix resulting from the difference equations described above became very ill conditioned, and the eigenfrequencies were very sensitive to small changes in the number and position of grid points, especially near the photosphere. Since we suspect that the shelf may be unphysical anyway, we chose to omit it. Two choices of truncation radius were used: the radius at which B changed sign¹ (for the 215 M_{\odot} and more massive models) or the radius at which the pressure scale height has a local minimum (applicable to all but the two lowest mass models presented). When the mass is low enough so that these radii do not exist below the photosphere, the entire MESA model is analysed, and in all such cases convergence is obtained.

4 RESULTS

4.1 Quasi-Adiabatic Calculations

First we describe the results obtained using ADIPLS. The seven lowest-frequency modes for our 464 M_{\odot} model are shown in Figure 4. Weighting the displacement δr by $\rho^{1/2}r$ shows where the energy of the mode is concentrated, in that ω^2 times the integral of the square of the plotted quantity gives the total energy.

Of particular note is that the first six modes discovered by ADIPLS are trapped in the shelf. The seventh mode is the true fundamental: its energy is concentrated in the core, where it has no nodes other than the centre, and it has an antinode at the base of the shelf (see §3). Care was taken to ensure that we were studying the same mode, as defined by these characteristics, across all models.

ADIPLS also reports the frequencies of these modes.

¹ B becomes positive again deep within the core, because it is $B - (P/\rho)$ rather than B that would vanish throughout an Eddington model in the limit $\beta \ll 1$. Despite the positivity of B in these deeper regions, they are unlikely to form the base of a wind before the substantial overlying mass is removed.

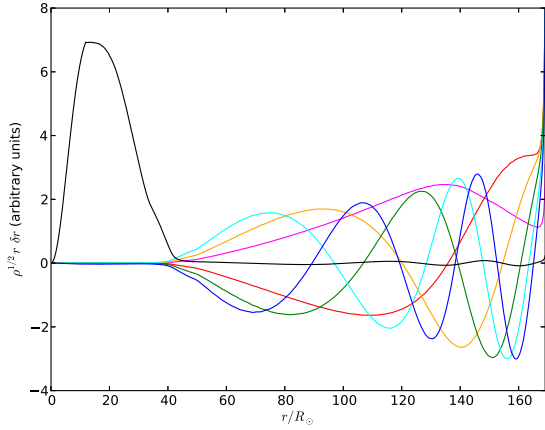


Figure 4. Plot of the lowest frequency adiabatic modes for the 464 M_{\odot} model. The curves show the square root of the mode kinetic energy per unit length, normalized independently. The modes have radial mode number n equal to 1 (red), 2 (orange), 3 (green), 4 (cyan), 5 (blue), 6 (magenta), or 7 (black), only the latter of which is not evanescent in the core.

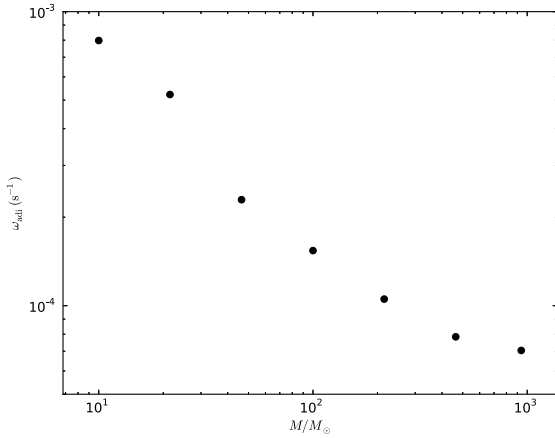


Figure 5. Adiabatic angular frequencies for the fundamental modes of our $Z = 0.02$ models. Note that the perturbation (18) alters these values only imperceptibly.

Those of the true fundamental for each model are compiled in Figure 5. For our most massive model the period is approximately one day. The real parts of the nonadiabatic frequencies computed as described in the next section differ from the ones shown by less than the widths of the symbols.

4.2 Nonadiabatic Calculations

Nonadiabaticity can arise from two primary mechanisms. First, the specific nuclear energy generation rate ϵ is sensitive to density and even more so to temperature, allowing the possibility for a fluid element's path through thermodynamic state space to result in net energy being put into the mode. In terms of the equilibrium model parameters, this effect is controlled by $\epsilon_T \equiv (\partial \log \epsilon / \partial \log T)|_{\rho}$ and $\epsilon_{\rho} \equiv (\partial \log \epsilon / \partial \log \rho)|_T$. The second consideration is the

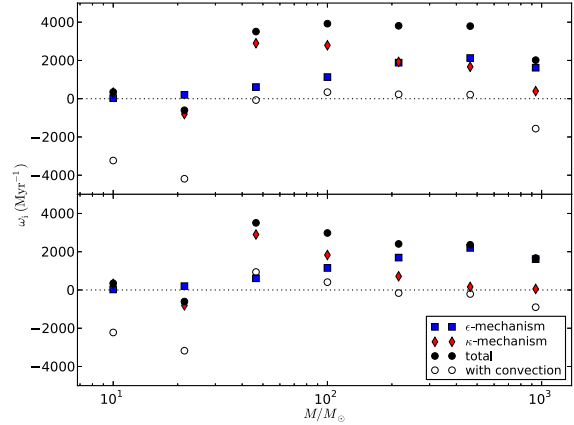


Figure 6. Growth rates in radians per million years for a range of masses. Negative values imply damping, i.e. linear stability. All models are ZAMS with initial metallicity $Z = 0.02$. The top panel shows the results cutting off the models where the Bernoulli constant becomes positive, while the bottom panel uses the local minimum of pressure scale height just interior to this radius. The ϵ -mechanism is more powerful for more massive stars, but its growth rate levels off at around 2000 Myr^{-1} for our models. The effect of opacity varies considerably in the intermediate-mass regime, but in the high-mass regime it is not a significant source of driving. Open circles denote adding in a quasi-adiabatic convective damping term.

Table 1. Growth rates as plotted in Figure 6

cutoff	M/M_{\odot}	Growth Rate (Myr^{-1})			
		ϵ	κ	total	convection
B	10	28	321	349	-3232
	21.5	201	-806	-605	-4186
	46.4	609	2900	3509	-72
	100	1132	2791	3923	342
	215	1883	1928	3811	230
	464	2127	1667	3794	213
	938	1620	396	2017	-1565
H_P	10	28	321	349	-2222
	21.5	201	-806	-605	-3175
	46.4	609	2900	3509	939
	100	1150	1829	2979	409
	215	1693	715	2408	-162
	464	2199	162	2361	-209
	938	1613	56	1669	-901

analogous one for opacity κ . The signs of κ_T and κ_{ρ} need not be positive, and so opacity effects can lead to either damping or growth.

When applying the numerics described in §2.2, we are free to artificially set any of ϵ_T , ϵ_{ρ} , κ_T , and κ_{ρ} to zero throughout the model. In this way we can separate the two effects. Figure 6 shows the growth rates for our models as given by nuclear energy generation effects, opacity effects, and the sum of the two. We show results corresponding to both cutoff criteria discussed in §3 – the sign change in the Bernoulli constant (top panel) and the local minimum in pressure scale height (bottom panel). The numbers are also listed in Table 1.

The effect of modulating the nuclear energy genera-

tion rate does indeed drive pulsations more strongly in more massive models, as expected. However, increasing the mass yields diminishing returns in this regard. Driving by the ϵ -mechanism is not affected by the choice of truncation radius at the base of the shelf (§3).

Opacity effects are somewhat more complicated, as one would expect given that varying the model's mass changes the relative locations of ionization regions. The $21.5 M_{\odot}$ model, for instance, is considerably damped by κ_T and κ_{ρ} , while more massive models' radial pulsations are driven by the same mechanism. Above about $50 M_{\odot}$ the models indicate that opacity effects contribute less to radial instability with increasing mass, especially when the models are truncated at the local minimum in pressure scale height.

The open symbols in Figure 6 include not only the sum of the two effects already discussed, but also a quasi-adiabatic work-integral correction due to convective zones having an effective bulk viscosity: in the most massive models, the pulsations are nearly homologous, meaning that the velocity field has more divergence than shear. It is well known that a monatomic ideal gas can have no bulk viscosity in the nonrelativistic or ultrarelativistic limits (e.g. Weinberg 1972), but we see no reason why turbulent convective viscosity should not. Here we use the same prescription as described in equations (11) and (12) of SQA. This viscosity cancels a significant fraction of the ϵ -mechanism driving in the higher-mass models.

We note that the ϵ -components of the nonadiabatic growth rates are similar to the values we get via a quasi-adiabatic work integral (cf. equation (8) from Shiode et al.), as should be expected given how well the adiabatic approximation holds in the inner core of these stars. The work integral predicts growth rates slightly larger than the ones we find, but all discrepancies are within 300 Myr^{-1} . For all models above $10 M_{\odot}$, the agreement between these methods for ω_i is better than 15 per cent.

5 NONLINEAR SATURATION

Appenzeller proposed that radial pulsations of very massive stars saturate in shocks that eject mass. His criterion for the onset of shocks was that the radial velocity at the photosphere become larger than the local sound speed. Papaloizou found in his own numerical calculations that shocks were not so easily formed, and saturation occurred without mass loss. Our view is closer to Papaloizou's, but we emphasize coupling to nonradial modes rather than radial overtones.

The largest growth rates we find are $\lesssim 10t_{\text{KH}}^{-1}$. Here t_{KH} is the Kelvin-Helmholtz time defined as by Goodman & Tan (2004), which asymptotes to $t_{\text{KH}} \approx 3000 \text{ yr}$ in the limit of very large masses.² On the other hand, the pulsation periods corresponding to the real parts of the frequencies shown in Figure 5 are $\lesssim 1 \text{ d}$, and we expect this to scale $\propto M^{-1/2}$ at higher masses. Thus the growth times are on the order of 10^5 pulsation periods. In this sense, the instabilities are extremely weak, even if the possibly stabilizing influence of convection is ignored.

² In order that the estimate of t_{KH} not be biased by the extended but almost massless shelf, we use for stellar radius the point at which the pressure scale height achieves its minimum value (R_H).

At one level, this is not a surprise. Whether caused by the ϵ - or κ -mechanism, pulsational instability operates by modulating the heat content of the star on the pulsation period. Thus, the smallness of the ratio $|\omega_i/\omega_r|$ reflects the disparity between the characteristic thermal and dynamical times of the star. We shall shortly argue that the smallness of the linear growth rate implies a small amplitude at nonlinear saturation.

This is not inconsistent with the relatively large amplitudes of oscillation of classical Cepheids ($\delta R/R \sim 0.1$) because the linear growth times are only ~ 100 pulsation periods in those stars (e.g., Castor 1971; Bono et al. 1999), and it is worth recalling why (e.g. Cox & Giuli 1968). Classical Cepheids are evolved stars with degenerate cores and a very large ratio of central to mean density. Consequently, the eigenfunction $\zeta(r) \equiv \delta r/r$ of the fundamental radial mode is very far from homologous, $\zeta(0)/\zeta(R) \sim \bar{\rho}/\rho(0) \ll 1$. The mode mass – the factor by which one multiplies the mean-square radial velocity at the surface to get the total energy in the mode – is many orders of magnitude smaller than the stellar mass of the star. In other words, for a given surface amplitude $\delta R/R$, the stored energy in the mode is much less than it would be if the pulsations were homologous, by a factor $\propto M_{\text{mode}}/M_*$. Since the driving regions for the κ -mechanism lie near the surface, the work integral is insensitive to the mode mass: it is of order $\Pi_0 \delta L \delta R/R$, where $\delta L/L \sim \delta R/R \sim -\delta T/T$ is the modulation of the surface luminosity and $\Pi_0 \equiv 2\pi\omega_r^{-1}$ is the pulsation period. Therefore the growth rate, which scales with the ratio of the work done per cycle to the stored energy in the mode, is $\sim (M_*/M_{\text{mode}})t_{\text{KH}}^{-1}$. The ϵ mechanism is negligible in Cepheids because the nuclear-burning regions are in shell sources near the centre, where $\delta \log T$ and $\delta r/r$ are much smaller than in the ionization zones.

As a quantitative example, we have used MESA to create a ‘Cepheid’ with the following parameters: $M_* = 5.7 M_{\odot}$, $R_* = 28.85 R_{\odot}$, $T_{\text{eff}} = 5900 \text{ K}$, and $L = 906 L_{\odot}$. For this model, $\bar{\rho}/\rho(0) = 6.2 \times 10^{-8}$, while $\zeta(0)/\zeta(R_*) = 3.3 \times 10^{-6}$ and $M_{\text{mode}}/M_* = 8.4 \times 10^{-5}$ for the fundamental radial mode computed with ADIPLS. By contrast, for the $938 M_{\odot}$ main-sequence model we find $\zeta(0)/\zeta(R) = 0.66$ and $M_{\text{mode}}/M_* = 0.061$. Thus the fundamental mode is approximately homologous and involves a significant fraction of the star's mass. We expect M_{mode}/M_* to be nearly constant and comparable to this for larger masses because of the similarity of these models to isentropic $n = 3$, $\Gamma_1 = 4/3$ polytropes. *Thus we also expect the growth rates of the fundamental radial mode to remain $\lesssim 10t_{\text{KH}}^{-1}$, as a consequence of the relatively homogeneous structure and homologous pulsation of these very massive main-sequence models, regardless of the details of the excitation and damping mechanisms.*

5.1 Saturation via 3-mode coupling

As a general rule, instabilities with smaller linear growth rates saturate at lower amplitudes. A simple model equation for the amplitude envelope $A > 0$ might be

$$\frac{dA}{dt} = \omega_i A - \nu A^{n+1}, \quad (20)$$

in which ω_i is the linear growth rate, while ν and n describe the nonlinearities. If ω_i , ν , and n are all positive, then equi-

librium is reached at $A_{\text{sat}} = (\omega_i/\nu)^{1/n}$. As noted above, pulsations in classical Cepheids grow relatively rapidly. Saturation in these stars and in RR Lyraes occurs via shocks and nonlinear modification of the conditions in the driving (ionization) zones (Christy 1966). Because of their much smaller dimensionless growth rates ($\omega_i/\omega_r \sim 10^{-6}$ instead of $\sim 10^{-3}$), the massive main-sequence stars considered here may saturate at lower amplitudes, where more delicate nonlinearities may be effective.

Dziembowski (1982) suggested that 3-mode coupling is responsible for saturation in dwarf Cepheids, and that this explains why they oscillate at lower amplitudes than do classical Cepheids. When the adiabatic fluid equations are derived from an action principle, 3-mode couplings occur in the Lagrangian density as terms cubic in fluid displacements (\mathcal{L}_3). When the growth rate of the primary (or ‘parent’) mode is small and the mode starts from a very small initial amplitude, it is these lowest-order nonlinearities that first come into play. The most important couplings are those that are resonant, meaning that the linear eigenfrequencies of the parent and daughter modes satisfy $\omega_p \approx \omega_{d1} + \omega_{d2}$, so that secular transfers of energy can occur.³ However, like any Hamiltonian that is truncated at third order in dynamical variables that can have either sign, the corresponding Hamiltonian density $\mathcal{H}_2 + \mathcal{H}_3$ cannot be positive definite unless the variables are restricted to small values. Thus higher-order contributions to \mathcal{L} and \mathcal{H} must dominate if the amplitudes pass some threshold, perhaps leading to shocks and a breakdown of the Hamiltonian description. Actually, even when the amplitudes remain small, dissipative (hence non-Hamiltonian) terms must be added to the equations of motion to describe the damping of the daughter modes. In application to pulsating stars, the growth rate of the parent is also represented by a non-adiabatic term. The daughter modes are often smaller in wavelength than the parent and therefore damped by radiative diffusion or other linear processes.

Landmark applications of 3-mode coupling to the saturation of stellar instabilities include those by Wu & Goldreich (2001) (to white dwarf/ZZ Ceti stars), as well as Schenk et al. (2002) and Arras et al. (2003) (to rapidly rotating neutron stars). Papaloizou (1973a) argued that pulsations of very massive stars driven by the ϵ -mechanism can saturate via direct resonant couplings: that is, the coupling of a quadratic or higher power of the fundamental mode to a *higher*-frequency radial *p* mode (overtone), so that $n\omega_f \approx \omega_d$ for some integer $n > 1$. Nonradial daughter modes offer many more possibilities for resonance, however: *g* modes are necessarily nonradial and have low frequencies, which is important for resonances of the type $\omega_p \approx \omega_{d1} + \omega_{d2}$ because the frequency of the fundamental, ω_f , is somewhat lower relative to the characteristic dynamical frequency $\omega_* \equiv (GM_*/R_*^3)^{1/2}$ than in less massive stars, the ratio ω_f/ω_* scaling as $M^{-1/2}$. Therefore we focus on couplings of this type. When the parent is the radial fundamental mode, the strongest 3-mode couplings are usually parametric subharmonic, meaning that the two daughter modes are two copies of the

same mode, with frequency $\omega_d \approx \omega_f/2$. The eigenfunction of a typical daughter mode is high-order – meaning that it has many nodes in radius and angle – but the square of the eigenfunction is nonnegative and hence may have a significant spatial overlap integral (3-mode coupling) with the nodeless radial fundamental. Parametric subharmonic destabilization of *g* modes and internal waves has been studied experimentally as well as theoretically (Benielli & Sommeria 1998, and references therein).

We use our most massive (938 M_\odot) model as an example, truncating it at $R_* \approx 46 R_\odot$, the minimum of the pressure scale height; this radius contains all but 3.4×10^{-6} of the total mass. Most of the star convects, but there is a radiative zone at $29 \lesssim r/R_\odot \leq 41$ containing $0.026M$. (There is also a second radiative zone at $r \geq 44 R_\odot$, but this contains only $1.4 \times 10^{-4}M$, so we ignore it when estimating coupling coefficients and damping rates.) The peak of the Brunt-Väisälä frequency is $N_{\text{max}} = 2.94\omega_*$, whereas the frequency of the fundamental radial mode is $\omega_f = 1.1446\omega_* \approx 7.116 \times 10^{-5} \text{ rad s}^{-1}$ according to ADIPLS (which computes only the real part), in good agreement with our non-adiabatic code. Thus there are many *g* modes with frequencies $\sim \omega_f/2$. Using the approximate WKB dispersion for high-order *g* modes,

$$\frac{\sqrt{l(l+1)}}{\omega_{ln}} \int N(r) \frac{dr}{r} \approx \pi(n - \frac{1}{2}), \quad (21)$$

and the profile of the Brunt-Väisälä frequency in the radiative zone, $N(r)$, we estimate that $n/l \approx 0.34$ for $\omega_{ln} \approx \omega_f/2$ and $l, n \gg 1$. For a non-rotating spherical star, so that the eigenfrequency is independent of spherical-harmonic order m , the number of mode frequencies in a given interval $\Delta\omega$ near $\omega_f/2$ that correspond to *g* modes of degree $l' \leq l$ scales as $0.17 l^2 \Delta \log \omega$ when $l \gg 1$. Inverting this, the minimum l at which one expects to find modes in the interval $\Delta\omega$ is

$$l_{\text{min}}(\Delta\omega) \approx 2.4 \left(\frac{\Delta\omega}{\omega} \right)^{-1/2}. \quad (22)$$

The distance $\Delta\omega$ from exact subharmonic resonance at which daughter modes can grow depends upon the linear damping rate of these modes, the amplitude of the parent, and the 3-mode coupling coefficient. For the damping time of high-order *g* modes by radiative diffusion, we apply (4.8) of Dziembowski (1982) to our 938 M_\odot model:

$$t_{\text{damp}} = \gamma_d^{-1} \approx 1.0 \left(\frac{30}{l} \frac{\omega_f}{2\omega} \right)^2 \text{ yr}. \quad (23)$$

We evaluate the 3-mode coupling coefficient from (A8) of Kumar & Goldreich (1989). Their formula assumes that the adiabatic exponent Γ_1 is constant and neglects the Eulerian perturbation to the gravitational potential, which, although essential for the eigenfrequency of the fundamental mode, is unimportant for the coupling since most of the stellar mass lies interior to the propagation region of the *g* modes in our case. We make the further approximation that the fundamental mode is exactly homologous, meaning that its radial displacement is given by $\delta r(r, t) = \zeta r \cos(\omega_f t)$, with ζ constant throughout the star [but growing slowly as $\exp(\omega_i t)$]. Finally we approximate the daughter-mode eigenfunctions using WKB, neglecting terms of relative order $(k_r H_P)^{-1}$, where $k_r \approx \sqrt{l(l+1)}N/\omega r$ is the radial

³ In resonance conditions such as this, all frequencies are understood to be real and nonnegative.

wavenumber and H_P the pressure scale height. We find that

$$\int \mathcal{H}_3 d^3 \mathbf{x} = \dots + \left(\frac{3\Gamma_1 - 1}{2} \right) \zeta \cos \omega_f t \int N^2 \delta r_d^2 dM. \quad (24)$$

Here ‘...’ represents all 3-mode coupling other than the one of interest, while $\delta r_d = q_d(t) \xi_{r,d}(r) Y_{lm}(\theta, \phi)$ is the radial displacement of the daughter mode, with time-dependent amplitude $q_d(t)$. To simplify the arithmetic, we set $\Gamma_1 = 4/3$, which would give a strictly homologous (but zero-frequency) fundamental mode; the mass-averaged value of Γ_1 in the 938 M_\odot model is closer to 1.37.

The integrand of (24) is twice the potential energy per unit mass of the g mode. The coupling term can therefore be treated as though it were a time-dependent correction to the linear dynamics of the daughter mode, whose amplitude evolves according to

$$\ddot{q}_d + 2\gamma_d \dot{q}_d + \omega_d^2 (1 + 3\zeta \cos(\omega_f t)) q_d = 0. \quad (25)$$

As usual with such Mathieu equations, if ζ and γ_d/ω_d are both small, then the solutions for $q_d(t)$ are sinusoidal but with envelopes varying as $\exp(st)$, with

$$s = -\gamma_d \pm \frac{3\zeta\omega_d}{4} \sqrt{1 - \left(\frac{4\Delta\omega_d}{3\zeta\omega_d} \right)^2}, \quad \Delta\omega_d \equiv \omega_d - \frac{1}{2}\omega_f. \quad (26)$$

Thus in order that the daughter mode should grow even at exact resonance ($\Delta\omega_d = 0$), we must have $\zeta > 4\gamma_d/3\omega_d$. On the one hand, since $\gamma_d \propto l^2$ according to (23), this sets an upper bound to the degrees of daughter modes that can be destabilized when the amplitude of the fundamental is $\delta R/R = \zeta$. On the other hand, l must be large enough so that it is probable to find eigenfrequencies within the range $|\Delta\omega_d| \leq 3\zeta\omega_d/4$ for which the square root in (25) is real. Thus in effect we must evaluate γ_d at the degree l_{\min} that is found by setting $\Delta \log \omega \approx \zeta$ in (22). Then $\gamma_d \propto l_{\min}^2 \propto \zeta^{-1}$, so that the requirement $\frac{3}{4}\zeta\omega_d > \gamma_d$ for growth leads to an inequality of the form $\zeta > C\zeta^{-1}$. Evaluating the numerical factor C , we find that the threshold for exciting daughter modes is approximately

$$\left(\frac{\delta R}{R} \right)_{\min} \approx 2.8 \times 10^{-3}, \quad l_d \approx 45. \quad (27)$$

Since the mode frequencies are sensitive to details of the stellar model, the occurrence of resonance is effectively probabilistic, and therefore the threshold for subharmonic instability will vary somewhat. In fact, for the particular model considered here, ADIPLS finds $\Delta\omega_d/\omega_d \approx 4 \times 10^{-4}$ at $l_d = 26$, which is some 20 times closer to resonance than would be expected from (22).

The threshold (27) of subharmonic instability involves only the current amplitude of the fundamental mode, not its rate of growth, ω_i . The latter is important for deciding whether the daughter modes can actually accept and dissipate energy from the parent faster than the nonadiabatic work integral increases that energy. Arras et al. (2003) state as a rule of thumb that the condition for this is simply $\gamma_d > \omega_i$, a regime they call ‘weak driving.’ Clearly this would suffice for nonlinear saturation of the unstable parent mode if a daughter mode could reach energy equipartition with the parent. In our case, the wavelength of the first daughters to go unstable is much smaller than the radius of the star, roughly by a factor $2/l$ when one accounts for both the radial and angular components of the wavenumber. Also

the mass of the g-mode propagation zone is only $0.026M$, whereas the mass of the fundamental mode is $0.061M$, as previously discussed. Therefore if a daughter mode at, say, $l_d = 45$ were to have the same energy as the fundamental, it would have a strain rate (spatial derivative of velocity) roughly $2\pi \times (l/2) \times \sqrt{0.061/0.026} \approx 4.6l$ times larger than the parent. At such a strain rate, the daughter mode would destabilize still other modes (granddaughters) and probably transfer energy to them more quickly than it could receive energy from the parent. Therefore equipartition is unlikely.

On the other hand, $\gamma_d \gg \omega_i$ in the present case, so that the rate of linear dissipation by daughter modes could balance the growth of the parent even if the daughters’ energies were well below equipartition with the parent. Because of the degeneracy of the eigenfrequencies in a non-rotating star, $2l_d + 1$ daughter modes grow at the same rate. When the average energy *per mode* reaches a value \bar{E}_d , the total linear dissipation rate becomes $2(2l_d + 1)\gamma_d \bar{E}_d$. Setting this equal to the rate at which the fundamental mode gains energy from its own linear instability, $2\omega_i E_f$, shows that saturation is possible when $\bar{E}_d/E_f \approx (2l_d + 1)^{-1}(\omega_i/\gamma_d)$. Evaluating this for $l_d = 45$, $\gamma_d^{-1} \approx 0.46 \text{ yr}$ [cf. (23)], and $\omega_i = (500 \text{ yr})^{-1}$ leads to $\bar{E}_d/E_f \approx 10^{-5}$. The ratio of strain rates is then

$$\frac{1}{2} \sqrt{\frac{\bar{E}_d}{E_f}} \times 4.6l_d \approx 0.3 \quad (l_d \approx 45) \quad (28)$$

(a factor of $1/2$ reflects the lower frequency of the daughters). Since this is less than unity, saturation is likely at daughter amplitudes too small to excite granddaughters.

We conclude that it is indeed likely that 3-mode coupling will saturate the growth of the fundamental radial mode. However, some caveats are in order regarding rotation, which we have so far neglected.

There are at least two rotational regimes to consider: slow and fast. Slow rotation at an angular velocity $\Omega \gtrsim l_d^{-1}\omega_*$ but $\ll N_{\max}$ will lift the degeneracy with respect to spherical-harmonic order m , while preserving the degree l as a useful approximate quantum number. Since there are more distinct eigenfrequencies, subharmonic resonance becomes possible at smaller l : (22) is replaced by $l_{\min} \approx 1.6(\Delta\omega/\omega)^{-1/3} \rightarrow 0.6\zeta^{-1/3}$. Otherwise following the same steps as before, the threshold of instability occurs at $\zeta \approx 5.4 \times 10^{-4}$ and $l_d \approx 20$ (both lower than before). Now a single, nondegenerate daughter mode first goes unstable, so the required balance at saturation if this daughter only is active becomes $2\gamma_d \bar{E}_d = 2\omega_i E_f$, and the ratio of strain rates (daughter:parent) works out to ≈ 3 instead of 0.3. Hence nonlinear coupling of the daughter to granddaughters may occur, limiting the energy of the former and complicating the analysis. On the other hand, the number of unstable daughters will increase rapidly ($\propto \zeta^{5/2}$) as the amplitude of the parent increases above the first subharmonic threshold, so without having analysed the situation carefully, we still expect saturation to occur.

By fast rotation, we mean fast enough so that inertial oscillations – approximately incompressible motions restored by Coriolis rather than buoyancy forces – can have resonant 3-mode couplings with the parent, as considered by Schenck et al. (2002) and Arras et al. (2003) for neutron stars. Since the maximum frequency of inertial oscillations is 2Ω , a necessary condition for subharmonic instability of

the fundamental mode is $\Omega > \omega_f/4$. In the $938 M_\odot$ model, this translates to $\Omega > 0.286\omega_*$, which is half or less than the mass-shedding limit for an $n = 3$ polytrope, depending how one defines ω_* for a nonspherical body (Hurley & Roberts 1964). Rapid rotation is not unreasonable for a body recently formed by fragmentation of an AGN accretion disk. Furthermore, ω_f/ω_* scales as $M^{-1/2}$ with increasing stellar mass.⁴ Unlike g modes, inertial oscillations propagate in convection zones, so that they may be destabilized throughout these (largely convective) massive stars. This is salient because we are not sure how the mass fraction of the radiative zones should scale at masses above $10^3 M_\odot$ and super-solar metallicities. Finally, we remark that even when the condition $\Omega > \omega_f/4$ is not satisfied, the imposition of rotation on vigorous convection will surely lead to magnetic fields, perhaps in rough equipartition with the convection, so that radial pulsations may couple nonlinearly to small-scale Alfvénic modes.

6 SUMMARY AND DISCUSSION

We have re-examined the stability of the fundamental radial mode of very massive main-sequence stars. Although nonradial and higher-order radial modes may also be unstable, we focus on the radial fundamental because collapse or explosion of these radiation-pressure-dominated objects would begin with this mode at linear order. In agreement with Shiode et al., we find that the linear growth rate is sensitive to turbulent convective damping. We have extended their results to higher masses at solar metallicity, and we have used a fully nonadiabatic rather than quasi-adiabatic method, which allows us to treat the κ -mechanism more reliably. The ϵ mechanism is more important for our most massive models we consider, however.

The linear growth rates remain uncertain not only because of the turbulent bulk viscosity, but also because of the tenuous (and possibly unphysical) envelopes possessed by all of our models above $100 M_\odot$. Nevertheless, the growth rate should in any case be extremely small, $\omega_i/\omega_r \sim \Pi_0/t_{KH}$, due to the relatively low central concentrations of these stars and the correspondingly large mode masses.

We have then argued from the smallness of the linear growth rate (in case this is positive) that the radial fundamental should saturate at a small amplitude due to any one of a number of weak nonlinearities. To support this claim, we have estimated the saturation amplitude that would result if parametric coupling to high-order g modes were the most important nonlinearity. For our most massive model, the estimate is $\delta R/R \approx 3 \times 10^{-3}$. Other nonlinear couplings may stop the growth at even smaller amplitudes, but those we identify would depend on uncertain parameters such as the star's rotation rate or magnetic field.

We conclude that thermally driven pulsations of the radial fundamental mode do not limit the main-sequence lifetimes of very massive stars. The tenuous outer envelopes of the more massive MESA models, however, which stem from an opacity bump at $\sim 10^5$ K, lead us to suspect that these stars would have powerful winds if the hydrostatic constraint were lifted, and that the mass-loss timescale (M_*/\dot{M}) may be much less than one million years, though necessarily longer than the Kelvin-Helmholtz timescale (≈ 3000 yr). The lower bound would be achieved only if all of the stellar luminosity were converted to the mechanical energy of a wind with vanishing asymptotic velocity at infinity.

ACKNOWLEDGEMENTS

This project made extensive use of the MESA stellar-evolution code and the ADIPLS asteroseismology package.

REFERENCES

- Appenzeller I., 1970, *A&A*, 9, 216
- Arras P., Flanagan E. E., Morsink S. M., Schenk A. K., Teukolsky S. A., Wasserman I., 2003, *ApJ*, 591, 1129
- Baumgarte T. W., Shapiro S. L., 1999, *ApJ*, 526, 941
- Benielli D., Sommeria J., 1998, *Journal of Fluid Mechanics*, 374, 117
- Bonanos A. Z., Stanek K. Z., Udalski A., Wyrzykowski L., Żebruń K., Kubiak M., Szymański M. K., Szweczyk O., Pietrzyński G., Soszyński I., 2004, *Astrophys. J.*, 611, L33
- Bono G., Marconi M., Stellingwerf R. F., 1999, *ApJS*, 122, 167
- Castor J. I., 1971, *ApJ*, 166, 109
- Chandrasekhar S., 1964, *ApJ*, 140, 417
- Christensen-Dalsgaard J., 2008, *ApSS*, 316, 113
- Christy R. F., 1966, *ApJ*, 144, 108
- Cox J. P., Giuli R. T., 1968, *Principles of stellar structure*. New York: Gordon and Breach
- Crowther P. A., Schnurr O., Hirschi R., Yusof N., Parker R. J., Goodwin S. P., Kassim H. A., 2010, *Mon. Not. R. Astr. Soc.*, 408, 731
- Dhanda Batra N., Baldwin J. A., 2014, *ArXiv e-prints*
- Dietrich M., Hamann F., Shields J. C., Constantin A., Heidt J., Jäger K., Vestergaard M., Wagner S. J., 2003, *ApJ*, 589, 722
- Dziembowski W., 1982, *Acta Astron.*, 32, 147
- Figer D. F., 2005, *Nature*, 434, 192
- Goodman J., Tan J. C., 2004, *ApJ*, 608, 108
- Gräfener G., Owocki S. P., Vink J. S., 2012, *A&A*, 538, A40
- Hamann F., Ferland G., 1999, *ARAA*, 37, 487
- Heney L., Vardya M. S., Bodenheimer P., 1965, *ApJ*, 142, 841
- Hurley M., Roberts P. H., 1964, *ApJ*, 140, 583
- Jiang Y.-F., Goodman J., 2011, *ApJ*, 730, 45
- Koen C., 2006, *Mon. Not. R. Astr. Soc.*, 365, 590
- Kumar P., Goldreich P., 1989, *ApJ*, 342, 558
- Matsuoka K., Nagao T., Marconi A., Maiolino R., Taniguchi Y., 2011, *A&A*, 527, A100
- Montero P. J., Janka H.-T., Müller E., 2012, *ApJ*, 749, 37
- Oey M. S., Clarke C. J., 2005, *Astrophys. J.*, 620, L43

⁴ Uniform rotation at the mass-shedding limit may set a lower limit to ω_f/ω_* because rotational energy behaves somewhat like gas pressure in the time-dependent virial theorem. Due to the central concentration of $n = 3$ polytropes, however, we estimate that this limit comes into effect only for $M \gtrsim 10^5 M_\odot$, where relativistic corrections must also be considered (Baumgarte & Shapiro 1999).

- Papaloizou J. C. B., 1973a, *Mon. Not. R. Astr. Soc.*, 162, 143
- Papaloizou J. C. B., 1973b, *Mon. Not. R. Astr. Soc.*, 162, 169
- Paxton B., Bildsten L., Dotter A., Herwig F., Lesaffre P., Timmes F., 2011, *ApJS*, 192, 3
- Paxton B., Cantiello M., Arras P., Bildsten L., Brown E. F., Dotter A., Mankovich C., Montgomery M. H., Stello D., Timmes F. X., Townsend R., 2013, *ArXiv e-prints*
- Rauw G., De Becker M., Nazé Y., Crowther P. A., Gosset E., Sana H., van der Hucht K. A., Vreux J.-M., Williams P. M., 2004, *A&A*, 420, L9
- Schenk A. K., Arras P., Flanagan É. É., Teukolsky S. A., Wasserman I., 2002, *Phys. Rev. D*, 65, 024001
- Schnurr O., 2012, in Drissen L., Rubert C., St-Louis N., Moffat A. F. J., eds, *Proceedings of a Scientific Meeting in Honor of Anthony F. J. Moffat Vol. 465 of Astronomical Society of the Pacific Conference Series, The Most Massive Stars*. p. 187
- Schwarzschild M., Härm R., 1959, *ApJ*, 129, 637
- Shiode J. H., Quataert E., Arras P., 2012, *Mon. Not. R. Astr. Soc.*, 423, 3397
- Weidner C., Kroupa P., 2004, *Mon. Not. R. Astr. Soc.*, 348, 187
- Weinberg S., 1972, *Gravitation and Cosmology: Principles and Applications of the General Theory of Relativity*. Wiley
- Wu Y., Goldreich P., 2001, *ApJ*, 546, 469

This paper has been typeset from a \LaTeX file prepared by the author.